

Searching for primordial black holes with stochastic gravitational-wave background in the space-based detector frequency band

Yi-Fan Wang,^{1,2,3,*} Qing-Guo Huang,^{4,5,6,7} Tjonnie G.F. Li,³ and Shihong Liao⁸

¹*Max-Planck-Institut für Gravitationsphysik (Albert-Einstein-Institut), D-30167 Hannover, Germany*

²*Leibniz Universität Hannover, D-30167 Hannover, Germany*

³*Department of Physics, The Chinese University of Hong Kong, Shatin, New Territories, Hong Kong*

⁴*CAS Key Laboratory of Theoretical Physics, Institute of Theoretical Physics, Chinese Academy of Sciences, Beijing 100190, China*

⁵*School of Physical Sciences, University of Chinese Academy of Sciences, No. 19A Yuquan Road, Beijing 100049, China*

⁶*Center for Gravitation and Cosmology, College of Physical Science and Technology, Yangzhou University, 88 South University Avenue, 225009, Yangzhou, China*

⁷*Synergetic Innovation Center for Quantum Effects and Applications, Hunan Normal University, 36 Lushan Lu, 410081, Changsha, China*

⁸*Key Laboratory for Computational Astrophysics, National Astronomical Observatories, Chinese Academy of Sciences, Beijing 100012, China*

Assuming that primordial black holes compose a fraction of dark matter, some of them may accumulate at the center of galaxy and perform a prograde or retrograde orbit against the gravity pointing towards the center exerted by the central massive black hole. If the mass of primordial black holes is of the order of stellar mass or smaller, such extreme mass ratio inspirals can emit gravitational waves and form a background due to incoherent superposition of all the contributions of the Universe. We investigate the stochastic gravitational-wave background energy density spectra from the directional source, the primordial black holes surrounding Sagittarius A* of the Milky Way, and the isotropic extragalactic total contribution, respectively. As will be shown, the resultant stochastic gravitational-wave background energy density shows different spectrum features such as the peak positions in the frequency domain for the above two kinds of sources. Detection of stochastic gravitational-wave background with such a feature may provide evidence for the existence of primordial black holes. Conversely, a null searching result can put constraints on the abundance of primordial black holes in dark matter.

I. INTRODUCTION

The recent direct detections of gravitational waves (GWs) by the LIGO and Virgo collaborations open a unique window to observe black holes (BHs) [1–8]. The event rate of binary BH merger at local Universe is estimated to be $53.2^{+58.5}_{-28.8} \text{ Gpc}^{-3} \text{ yr}^{-1}$ from the detections [9]. Among the GW events, the relatively large mass of the first detection ($\sim 30 M_\odot$), GW150914, has stimulated discussions that the binary BHs of GW150914 could be of primordial origin, instead of products of stellar evolution [10–13]. Ref. [12] shows that the binary stellar-mass primordial BHs coalescence scenario can give the correct order of magnitude of event rate, if the abundance of primordial BHs in dark matter is $\sim 10^{-3}$.

Primordial BHs are a long hypothesized candidate for dark matter [14–17]. Assuming all the primordial BHs have the same mass, a variety of observations from astronomy and cosmology have given constraints on the primordial BH abundance in dark matter, for example, gravitational lensing of stars and quasars, dynamics of dwarf galaxies, large scale structure formation and accretion effects on the cosmic microwave background (CMB) (see Refs. [18–21] and references therein). The possibility that all the dark matter are primordial BHs with the

same mass has been ruled out given all the constraints aforementioned (but see, e.g., Ref. [22]). Nevertheless, it is still interesting to consider the scenario where primordial BHs compose a part of dark matter and propose new methods to seek for evidence of primordial BHs or constrain their abundance in dark matter, especially leveraging the newly opened GW window [23, 24].

In this work, we investigate the scenario in which primordial BHs constitute a fraction of dark matter in the galactic center. Astrophysical observations (see, e.g., Refs. [25, 26] for a review) indicate that massive BHs with mass $10^3 M_\odot - 10^9 M_\odot$ are ubiquitous and reside at the center of almost every massive galaxy. If some fraction of dark matter is composited by primordial BHs, they should perform a prograde or retrograde orbit against the gravity pointing towards the galactic center exerted by the central massive BH, and such a system becomes the so-called extreme mass ratio inspiral (EMRI) system whose mass ratio is usually larger than 10^5 [27]. EMRIs are one of the important scientific targets of space-based GW detector, such as Laser Interferometer Space Antenna (LISA) which is anticipated to be launched in the 2030s¹. Once detected, the GW signals from EMRIs can provide valuable information such as event rate estimation [27, 28] and tests of general relativity [29, 30].

* yifan.wang@aei.mpg.de

¹ <https://www.elisascience.org/>

The focus of our work is the stochastic gravitational-wave background (SGWB) energy density spectrum from the EMRI system consisting of a massive BH at the galactic center and a subsolar mass primordial BH. SGWB is an incoherent superposition of numerous GWs, including those too weak to be detected individually [31–35] or having an intrinsic stochastic nature, such as the primordial GW which is generated by quantum fluctuations in the early Universe. The SGWB from binary stellar-mass primordial BH coalescence is calculated by Refs. [36–39] and, in particular, Ref. [37] shows that the null result of SGWB in the LIGO frequency band ($\sim [10, 1000]$ Hz) has given the most stringent constraints on the abundance of primordial BH as dark matter in the mass range $[1, 100] M_\odot$. In the LISA frequency band, Refs. [40, 41] have considered the stochastic background from subsolar mass primordial BHs inspiraling to Sagittarius A*, i.e., the central massive BH of the Milky Way. Our work will expand the study of Refs. [40, 41] in the following two aspects. First, we calculate the SGWB energy density spectrum in the frequency domain, i.e., $\Omega_{\text{GW}}(\nu)$ from the primordial BHs surrounding Sagittarius A*. Second, we investigate the complete SGWB contributions from extragalactic sources by modeling the event rate of primordial BH EMRIs throughout the cosmic redshift.

The rest of the paper is arranged as follows. In Section II we model the primordial BHs density profile around a massive BH, and apply this relation to the Sagittarius A* in the Milky Way to derive the SGWB energy density spectrum. We proceed to model the number density of massive BHs at different redshift epochs and calculate the SGWB spectrum from extragalactic sources in Section III. We forecast the ability of LISA for detecting the SGWB signal or, if there is a null result, constraining the abundance of primordial BHs in dark matter in Section IV. The results show that LISA can probe the existence of primordial BHs with mass range $[10^{-8}, 1] M_\odot$ and constrain the abundance of primordial BH with $1M_\odot$ to be 10^{-9} in the optimal case where the dark-matter spike scenario with a steeper initial power index $\gamma = 2$ is valid. The main uncertainty is subject to the value of the dark-matter initial power index γ . We summarize the conclusions in Section V. Throughout this work we assume the mass distribution of primordial BHs is a delta function due to the uncertainty of the primordial BH population. Therefore the results should be seen as being from the primordial BHs with a representative mass. Actually, as will be shown in the following, the mass of primordial BHs only serves as a scaling factor for the amplitude of the resulting SGWB spectra and the shape of spectra only depends on the mass of the central massive BHs.

II. THE STOCHASTIC GRAVITATIONAL-WAVE BACKGROUND FROM SAGITTARIUS A*

A. Primordial Black Holes Density Profile

To model the event rate of primordial BH EMRIs, we first infer the primordial BH mass density at the galactic center. Since we expect that primordial BHs compose a part of dark matter, it is natural to use the dark-matter density profile to characterize the primordial BH mass density around the central massive BH.

For an initial dark-matter density profile with the following power law form

$$\rho(r) = \rho_0 \left(\frac{r_0}{r} \right)^\gamma, \quad (1)$$

where ρ_0 and r_0 are halo parameters and to be determined, γ is the power index, r is the radius of dark matter, Ref. [42] suggests that the adiabatic growth of the central massive BH can enhance the surrounding dark-matter density at galactic center and form a spike distribution, i.e., the halo will end up with the following density [42, 43]

$$\rho_{\text{sp}}(r) = \rho_R \left(1 - \frac{4R_s}{r} \right)^3 \left(\frac{R_{\text{sp}}}{r} \right)^{\gamma_{\text{sp}}}, \quad (2)$$

where the power index is enhanced from the initial value by $\gamma_{\text{sp}} = (9 - 2\gamma)/(4 - \gamma)$, the halo parameter $\rho_R = \rho_0(R_{\text{sp}}/r_0)^{-\gamma}$ with R_s being the Schwarzschild radius of the central massive BH, $R_{\text{sp}}(\gamma, M_{\text{MBH}}) = \alpha_\gamma r_0 (M_{\text{MBH}}/(\rho_0 r_0^3))^{1/(3-\gamma)}$ is the radius to which the dark-matter spike extends, α_γ is derived numerically for different γ in Ref. [42]. For an initial Navarro-Frenk-White (NFW) profile [44] with $\gamma = 1$, the final spike has a index $\gamma_{\text{sp}} = 7/3$, thus significantly boosting the inner profile around the central massive BH.

To connect ρ_0 and r_0 with the massive BH's property, we employ the relation among the dark-matter halo virial mass M_{vir} , the concentration parameter $c_{\text{con}} \equiv r_{\text{vir}}/r_0$ where r_{vir} is the halo virial radius, and the mass of massive BH M_{MBH} . The relation of $c_{\text{con}} - M_{\text{vir}}$ for NFW profile is given by Ref. [45]

$$\log c_{\text{con}} = a + b \log \frac{M_{\text{vir}}}{10^{12} h^{-1} M_\odot}, \quad (3)$$

where $a = 0.520 + 0.385 \exp(-0.617z^{1.21})$ and $b = -0.101 + 0.026z$ are numerical factors at redshift z . The parametrized formula Eq. (3) is obtained by numerically fitting to a suite of N-body simulations for NFW profile with *Planck* 2013 cosmological parameters [46] in the redshift range $[0, 5]$.

The mass of the central massive BHs has a correlation with a few characteristic quantities of the host galaxy, such as the velocity dispersion σ in the spheroidal region and the total mass of the host galaxy, indicating a coevolution history with the whole galaxy. By employing the

observational $M_{\text{MBH}} - \sigma$ relation and using the quasar luminosity function to link σ with the halo mass, Ref. [47] gives a parametrized relation between the massive BH's mass M_{MBH} and the host dark-matter halo's virial mass M_{vir} ,

$$\log \left(\frac{M_{\text{MBH}}}{10^8 h^{-1} M_{\odot}} \right) = (-2.66 \pm 0.33) + (1.39 \pm 0.22) \times \log \left[\beta^3 H(z) \left(\frac{M_{\text{vir}}}{10^{13} h^{-1} M_{\odot}} \right) \right]. \quad (4)$$

Here $H(z) = H_0 \sqrt{\Omega_m(1+z)^3 + \Omega_\Lambda}$ is the Hubble parameter at redshift z , Ω_m and Ω_Λ are the matter and dark energy fractional densities, respectively. β is a ratio between the dark-matter halo's circular velocity and virial velocity, whose value is of order unity. Eq. (3) together with Eq. (4) can fix the corresponding coefficients of NFW density profile and NFW induced spike profile given the mass of massive BH.

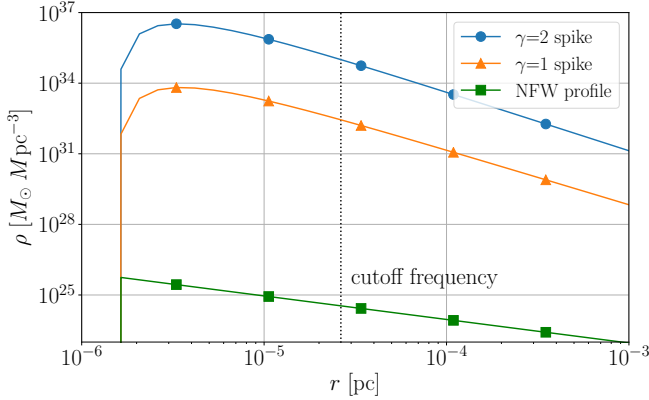


FIG. 1: Dark matter density profile around a massive BH with mass $4 \times 10^6 M_{\odot}$. The blue and orange solid curves show the spike profile for power index $\gamma = 2$ and $\gamma = 1$, respectively. As a comparison, the NFW dark-matter profile is also plotted. The dark-matter density profile at galactic center is boosted significantly for the $\gamma = 1$ spike profile compared with the NFW profile. The $\gamma = 2$ spike has even larger density than $\gamma = 1$ by three orders of magnitude. The vertical dashed line represents the orbital radius where the GW frequency is 10^{-5} Hz which is the lower cutoff frequency of the LISA sensitive band.

Fig. 1 shows the dark-matter spike profile around a massive BH with mass $4 \times 10^6 M_{\odot}$. Given the uncertainty of the initial profile power index, we choose two values for γ , $\gamma = 1$ for NFW profile and $\gamma = 2$ representing a steeper profile for an optimistic result. We observe that the dark-matter density near the galactic center is boosted significantly for the $\gamma = 1$ spike profile compared with the NFW profile. The $\gamma = 2$ spike has even larger density than $\gamma = 1$ by three orders of magnitude.

In Fig. 1, the vertical dashed line represents the radius where the emitted GW frequency is 10^{-5} Hz where we have assumed primordial BHs perform circular motion. Therefore, the region of interest for the LISA frequency band is between $4R_s$ as indicated by Eq. (2), and the dashed line.

B. Stochastic Gravitational-Wave Background Spectrum

The fractional energy density spectrum of SGWB is defined as

$$\Omega_{\text{GW}} = \frac{\nu}{\rho_c} \frac{d\rho_{\text{GW}}}{d\nu}, \quad (5)$$

where $d\rho_{\text{GW}}$ is the gravitational-wave energy density in the frequency band $[\nu, \nu + d\nu]$, $\rho_c = 3H_0^2 c^2 / 8\pi G$ is the critical energy to close the Universe, G is the gravitational constant, c is the speed of light.

The local energy density is related to the GW energy flux by $\rho_{\text{GW}}(\nu) = F_{\text{GW}}(\nu)/c$. $F_{\text{GW}}(\nu)$ from Sagittarius A* can be derived by taking the integral of the density of primordial BH EMRI with respect to the orbital radius r ,

$$F_{\text{GW}}(\nu) = \int \frac{f_{\text{PBH}} \rho_{\text{DM}}(r; M_{\text{MBH}})}{m_{\text{PBH}}} \frac{dE/dt(r; M_{\text{tot}}, \eta)}{d_L^2} r^2 dr, \quad (6)$$

where d_L is the luminosity distance from sources to GW detectors, $\rho_{\text{DM}}(r; M_{\text{MBH}})$ is the dark-matter density at radius r to the center given M_{MBH} , m_{PBH} and f_{PBH} are the primordial BH mass and abundance, $\eta \equiv m_{\text{PBH}} M_{\text{MBH}} / (m_{\text{PBH}} + M_{\text{MBH}})^2$ is the symmetric mass ratio, $M_{\text{tot}} \equiv m_{\text{PBH}} + M_{\text{MBH}}$ is the total mass of the primordial BH EMRI system. To the leading order, GW power can be calculated by the quadrupole formula [48, 49],

$$\frac{dE}{dt}(r; M_{\text{tot}}, \eta) = \frac{32}{5} \frac{G^4}{c^5} \eta^2 \left(\frac{M_{\text{tot}}}{r} \right)^5. \quad (7)$$

The radius r can be equivalently replaced by the GW frequency ν under the assumption of Keplerian motion,

$$r(\nu, M_{\text{tot}}) = \left[\frac{(GM_{\text{tot}})^{1/2}}{\pi(1+z)\nu} \right]^{\frac{2}{3}}, \quad (8)$$

where the factor of $(1+z)$ accounts for the cosmological expansion and the GW frequency ν is twice of the orbital frequency. From Eq. (8) a differential relation can be derived,

$$\frac{d}{d\nu} = -\frac{2\pi}{3} \frac{1+z}{(GM_{\text{tot}})^{1/2}} r^{5/2} \frac{d}{dr}. \quad (9)$$

Applying Eq. (9) to Eq. (6) and using the condition $M_{\text{MBH}} \gg m_{\text{PBH}}$, the differential GW power from Sagittarius A* is

$$\frac{dF_{\text{GW}}}{d\nu}(\nu) = \frac{64\pi}{15} \frac{(1+z)G^{7/2}}{c^5} \frac{f_{\text{PBH}} \rho_{\text{DM}} m_{\text{PBH}} M_{\text{MBH}}^{5/2}}{r^{1/2} d_L^2}, \quad (10)$$

Therefore the SGWB energy density spectrum is

$$\Omega_{\text{GW}}^{\text{SgrA}^*}(\nu) = \frac{\nu}{\rho_c} \frac{64\pi G^{7/2}}{15c^6} \frac{f_{\text{PBH}} m_{\text{PBH}} M_{\text{MBH}}^{5/2} \rho_{\text{DM}}}{r^{1/2} d_L^2}. \quad (11)$$

The mass of Sagittarius A* located at the center of the Milky Way is $\sim 4 \times 10^6 M_\odot$ and the distance d_L is ~ 8 kpc. Substitute the values to Eq. (11), the SGWB result is shown in Fig. 2 with $m_{\text{PBH}} = 1 M_\odot$ and $f_{\text{PBH}} = 1 \times 10^{-8}$. Note that the term $m_{\text{PBH}} f_{\text{PBH}}$ in Eq. (11) only serves as an overall scaling factor. We showcase two choices of the initial dark-matter profile power index, $\gamma = 1$ and 2 , respectively. As a comparison, the LISA sensitivity curve of SGWB for the six links, 5 million km arm length configuration and 5 year mission duration (the optimal case) is plotted [50, 51].

The figure shows that the amplitude of SGWB with $\gamma = 2$ is larger than that with $\gamma = 1$ by three orders of magnitude, inheriting from the three order of magnitude difference of the dark-matter halo density as shown in Fig. 1. Another feature is that the SGWB peaks at 3×10^{-4} Hz, which is determined by the mass of the central massive BH given the dark-matter spike distribution.

It should also be noted that the SGWB from Sagittarius A* is a directional signal, but the sensitivity curve is for isotropic SGWB. Therefore the comparison only serves as an order of magnitude estimation due to the lack of a sensitivity curve of space-based detectors for a directional background, but note that the technique of GW radiometer and the sensitivity for a directional stochastic background for LIGO have been proposed and calculated by Refs. [52]. The search for persistent GW signals from pointlike sources has been performed by Advanced [53, 54] and Initial LIGO and Virgo [55]. Especially, using the data from the first and second observational runs of Advanced LIGO and Virgo, the upper limits for GW strain amplitude have been given for three sources with targeting directions: Scorpius X-1, Supernova 1987 A and the Galactic Center, respectively. Refs. [56, 57] have considered the anisotropic SGWB search with space-based detectors. However, a specialized investigation for directional SGWB from primordial BH EMRIs at the Galactic center has not been achieved in the context of space-based GW detectors. We thus leave the relevant study as a future work.

III. THE STOCHASTIC GRAVITATIONAL-WAVE BACKGROUND FROM EXTRAGALACTIC SOURCES

A. Massive Black Hole Population

To model the massive BH population throughout the cosmic history, we employ the dark-matter halo mass function and the $M_{\text{MBH}} - M_{\text{vir}}$ relation which is characterized by Eq. (4). We choose the halo mass function in Ref. [58] which calibrates with a suite of cosmological N-body simulations and takes the finite box size and

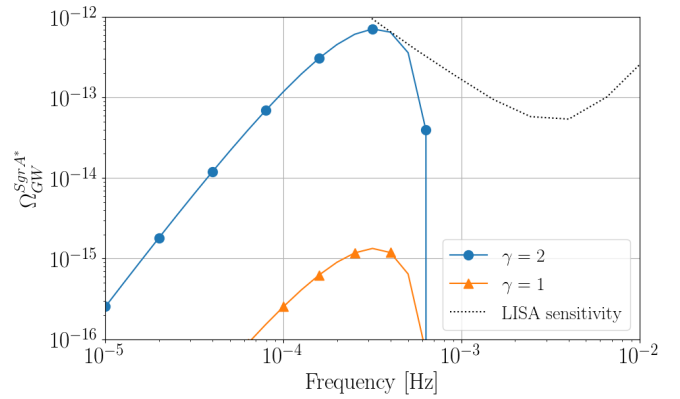


FIG. 2: The SGWB energy density spectra of primordial BH EMRIs surrounding Sagittarius A*, i.e., the massive BH at the center of Milky Way. The mass of primordial BH is chosen to be $m_{\text{PBH}} = 1 M_\odot$ and the abundance in dark matter is $f_{\text{PBH}} = 10^{-8}$. For the initial dark-matter profile power index, $\gamma = 2$ and $\gamma = 1$ are chosen for illustration. Both SGWB results peak at the frequency 3×10^{-4} Hz which is determined by the mass of the massive BH. The amplitude with $\gamma = 2$ is larger than $\gamma = 1$ by three orders of magnitude, inheriting from the three order of magnitude difference of the dark-matter halo density. The LISA sensitivity curve for detecting isotropic SGWB is also plotted for a qualitative comparison since the SGWB from Sagittarius A* is a directional signal. The sensitivity curve is for the optimal configuration of LISA which has six links with 5 million km arm length and a 5 year mission duration.

the cosmic variance effects into account. In the actual practice this halo mass function is generated through invoking the Reed07 model in the python package *hmf* (an acronym for “halo mass function”) [59], where the cosmological parameters are set to be the value of the *Planck* satellite’s 2018 results [60]. Reed07 model is shown to be valid up to redshift $z \sim 30$ and for halos with masses $10^{5-12} h^{-1} M_\odot$ [58], which is sufficient for our purpose.

Fig. 3 shows our results of the number density $dn/d \ln M_{\text{MBH}}$ for massive BHs in different redshifts. Since astronomical observations have confirmed the existence of massive BHs with $\sim 10^4 M_\odot$ (for example see Ref. [61]), we will consider the SGWB spectrum from the massive BHs in the mass range $[10^4, \sim 10^9] h^{-1} M_\odot$ as a fiducial model. The upper mass limit is determined by the condition that the emitted GWs are in the LISA sensitive band and $\sim 10^9 M_\odot$ is sufficient for this purpose.

B. Stochastic Gravitational-Wave Background Spectrum

The complete SGWB contribution can be obtained by taking the sum from the EMRIs of all extragalactic mas-

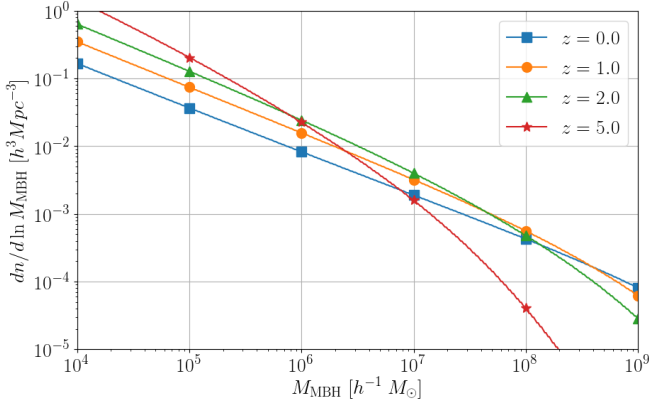


FIG. 3: The solid curves represent the number density of massive BH at different redshifts which is derived from Reed07 dark-matter halo mass function. We will consider the SGWB spectrum from the massive BHs in the mass range $[10^4, \sim 10^9] h^{-1} M_\odot$ as a fiducial model.

sive BHs

$$\Omega_{\text{GW}}(\nu) = \frac{\nu}{\rho_c} \frac{4\pi}{c} \iint \frac{dF_{\text{GW}}}{d\nu} \frac{dn}{dM_{\text{MBH}}} dM_{\text{MBH}} \chi^2 d\chi, \quad (12)$$

where dn/dM_{MBH} is the number density of massive BHs and χ is the sources' comoving distance. Combining Eq. (10) and Eq. (12) yields

$$\Omega_{\text{GW}}(\nu) = f_{\text{PBH}} m_{\text{PBH}} \frac{\nu}{\rho_c} \frac{256\pi^2 G^{7/2}}{15c^7} \times \int \frac{dz}{(1+z)H(z)} \int \frac{\rho_{\text{DM}} M_{\text{MBH}}^{5/2}}{r^{1/2}} \frac{dn}{dM_{\text{MBH}}} dM_{\text{MBH}}. \quad (13)$$

As a fiducial model, we consider the sources in the redshift range $[0, 5]$. Contributions from higher redshift can be negligible as will be indicated in Section III D.

With $m_{\text{PBH}} = 1 M_\odot$ and $f_{\text{PBH}} = 10^{-8}$, the results of extragalactic SGWB with $\gamma = 2$ and $\gamma = 1$ are shown in Fig. 4. The results from Sagittarius A* are also replotted for comparison. The extragalactic SGWB peaks at a higher frequency ($\sim 4 \times 10^{-2}$ Hz), due to the contributions from BHs less massive than Sagittarius A*.

Note that the extragalactic SGWB is an isotropic signal, and thus can be compared with the LISA sensitivity curve directly. It shows that the amplitude of extragalactic SGWB for $\gamma = 2$ already reaches the detectable zone, which means that the future LISA searching results can probe the abundance of $1 M_\odot$ primordial BHs to be as low as $\sim 10^{-9}$ for the $\gamma = 2$ case. The amplitude of $\gamma = 1$ SGWB is smaller by three orders of magnitude due to a smaller dark-matter density profile.

The main uncertainty comes from the dark-matter initial profile power index. Future astrophysical progress on understanding the dark-matter profile at galactic center can shed light on a more robust prediction on the primordial BH EMRIs event rate. Conversely, future GW search with space-based detectors can also be beneficial for study for the dark-matter profile.

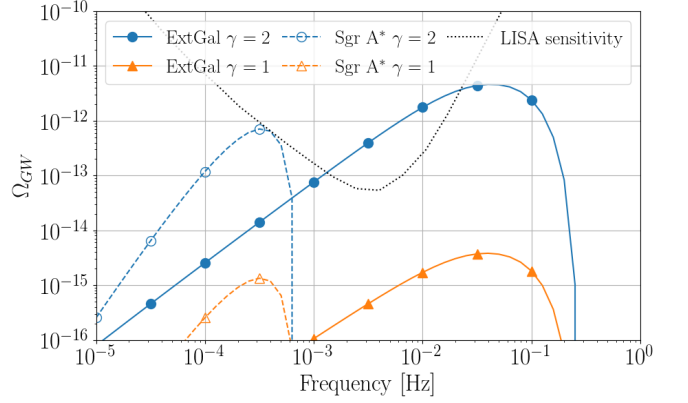


FIG. 4: The SGWB spectra from primordial BH EMRIs surrounding Sagittarius A* (“Sgr A*”) and the extragalactic massive BHs (“ExtGal”) in the redshift range $[0, 5]$. The mass of the primordial BH is assumed to be $1 M_\odot$ and the abundance in dark matter is 10^{-8} . The dark-matter initial profile power index is chosen to be $\gamma = 1$ and $\gamma = 2$, respectively. The $\gamma = 2$ extragalactic SGWB already reaches the detectable zone of LISA.

C. Density Enhancement due to Gravitational-Wave Dissipation

Another consideration is that the orbit of inspiraling primordial BHs will gradually decay due to GW dissipation. As a consequence, the primordial BH density profile gets further concentrated. To quantify this effect, we notice that astrophysical spectroscopy surveys have confirmed that the first galaxies form at redshift $z \gtrsim 10$ (~ 13 Gyr from now) [62]. Therefore we make the extreme assumption that all the primordial BHs EMRIs start to decay at $z = 10$, thus the decay duration equals to ~ 13 Gyr, to obtain an upper limit of the dark-matter density profile after concentration.

The relation among the orbital decay duration Δt , the final orbit radius r_f and the initial radius r_i is given by Refs. [48, 49] as follows

$$\Delta t = \frac{5}{256} \frac{c^5}{G^3} \frac{1}{\eta M_{\text{tot}}^3} (r_i^4 - r_f^4). \quad (14)$$

Let $\Delta t = 13$ Gyr and employ the mass conservation relation ²

$$\rho_f(r_f) = \frac{r_i^2}{r_f^2} \rho_i(r_i), \quad (15)$$

the enhanced density profile ρ_f can be determined from the initial dark-matter profile ρ_i which is assumed to the spike distribution.

² We have numerically verified that the mass loss due to GW dissipation is negligible by comparing the GW energy with the mass energy of primordial BHs.

For comparison, we also consider a less optimistic case where the orbital decay duration Δt is an average of a flat distribution which ranges from zero to 13 Gyr, i.e., the primordial BH final orbital radius after GW dissipation r_f can be determined by r_i with the following expression

$$r_f = \int_0^{13 \text{ Gyr}} \left(r_i^4 - \frac{256 G^3}{5 c^5} \eta M_{\text{tot}}^3 \Delta t \right)^{1/4} d\Delta t / 13 \text{ Gyr}. \quad (16)$$

However, we find numerically that the relative difference of the resulting SGWB spectra between the most optimistic case (i.e., $\Delta t = 13$ Gyr) and the less-optimistic case is negligibly small and at most $\mathcal{O}(10\%)$; therefore we will only consider the most optimistic case in the following as a representative of the GW dissipation effect.

Choosing $\gamma = 2$, the fiducial SGWB result without density enhancement for $m_{\text{PBH}} = 1M_\odot, f_{\text{PBH}} = 10^{-8}$ and the SGWB spectra with density enhancement for $m_{\text{PBH}} = 1M_\odot, 10^{-4}M_\odot$ and $10^{-8}M_\odot$, respectively, are shown in Fig. 5. For the enhanced SGWB results, the primordial BH abundance is modified accordingly to keep $m_{\text{PBH}}f_{\text{PBH}} = 10^{-8}$. Since GW dissipation makes primordial BHs get concentrated and closer to the center, the amplitude of SGWB spectra gets boosted and the frequency of the peak changes to $\sim 10^{-1}$ Hz. As the mass of primordial BHs decreases, the amplitude boost becomes more significant. The amplitude for $m_{\text{PBH}} = 10^{-8}M_\odot$ is larger than the fiducial result by one order of magnitude. This can be expected from Eq. (14) that a smaller value of symmetric mass ratio η leads to a more significant orbital decay.

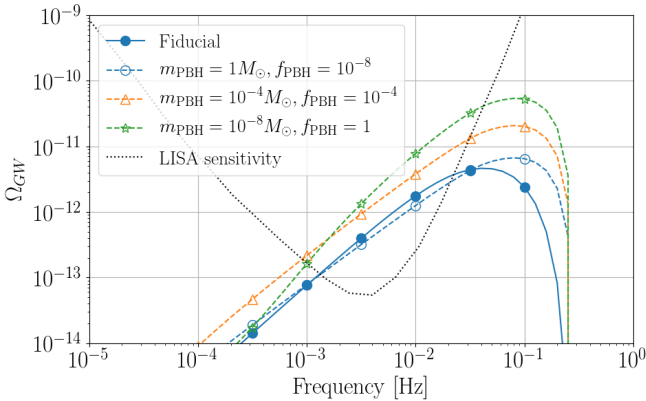


FIG. 5: A comparison between the SGWB spectra with and without primordial BH density enhancement effect due to GW dissipation. The fiducial model is calculated from the $\gamma = 2$ dark-matter spike distribution for $m_{\text{PBH}} = 1M_\odot, f_{\text{PBH}} = 10^{-8}$. The three dashed lines are from the $\gamma = 2$ enhanced dark-matter spike distribution due to GW dissipation. The mass and abundance parameters are so chosen to keep $m_{\text{PBH}}f_{\text{PBH}} = 10^{-8}$.

D. Modeling Systematics of the Massive Black Hole Population

To investigate the systematics on modeling the extragalactic massive BH population, we vary the redshift integral limits, the lower mass of massive BHs and the massive BH population model, respectively, and plot the corresponding SGWB spectra. The results are shown in Fig. 6. All SGWB spectra are calculated from $\gamma = 2$ dark-matter spike distribution and $f_{\text{PBH}} = 10^{-8}$, $m_{\text{PBH}} = 1M_\odot$.

1. The Redshift Limits of the Integral

The left column of Fig. 6 shows the SGWB component contributions from different redshift ranges, $[0, 1]$, $[1, 3]$, and $[3, 5]$, respectively. The fiducial result is the sum, i.e., obtained from the redshift range $[0, 5]$. We can see that the contribution from $z \in [3, 5]$ is subdominant and accounts for at most 10% of the fiducial result. We thus conclude that the choice of 5 for the redshift upper limit is sufficient to capture the dominant contribution.

2. The Lower Mass Cutoff of the Massive Black Holes

As mentioned, we chose $10^4 h^{-1}M_\odot$ to be the minimum mass of massive BHs to account for the existence of such massive BHs from astronomical observations. Nevertheless we change this value to $10^5 h^{-1}M_\odot$ to investigate the contribution from different mass ranges. The result is shown in the middle column of Fig. 6. Compared with the fiducial result whose lower mass cutoff is $10^4 h^{-1}M_\odot$, the result shows that the SGWB contributed by $[10^4, 10^5] h^{-1}M_\odot$ massive BHs is mainly in the relative high frequency range $[\sim 10^{-2}, \sim 10^{-1}]$ Hz. Therefore the shape of the SGWB spectrum, especially the frequency of the peak, can provide information of the underlying massive BH population.

3. The Population Model of Massive Black Holes

A third investigation is to substitute the massive BH population model derived from the Reed07 dark-matter halo mass function to that proposed by Refs. [63–66] accounting for the massive BHs formed from population III star seeds. The number density of massive BHs of this model is

$$\frac{dn}{d \log M_{\text{MBH}}} = 0.005 \left(\frac{M_{\text{MBH}}}{3 \times 10^6 M_\odot} \right)^{-0.3} \text{Mpc}^{-3} \quad (17)$$

The right column of Fig. 6 presents the results. It shows that the amplitude of the peak is one order of magnitude smaller than the fiducial model. This is because the number density of massive BHs with mass $[10^4, 10^6] h^{-1}M_\odot$

from Eq. (17) is less than that from the Reed07 derived population.

The above investigations give a quantitative measurement about the effect on SGWB spectra from different modeling systematics of extragalactic massive BH, which can be improved in the future once a better understanding of the population of massive BHs is obtained. In addition, the future SGWB search with space-based detectors can serve as a tool to probe the population information of massive BHs.

IV. CONSTRAINTS ON PRIMORDIAL BLACK HOLE ABUNDANCE

By comparing the SGWB spectrum with the LISA sensitivity and applying the condition

$$\Omega_{\text{GW}}(\nu; m_{\text{PBH}}, f_{\text{PBH}}) \leq \Omega_{\text{GW}}^{\text{LISA sensitivity}}, \quad (18)$$

the upper limit on primordial BH abundance $f_{\text{PBH}}^{\text{max}}$ can be obtained for a null searching result. In Fig. 7, we plot the results for different primordial BH masses from the models of $\gamma = 1$, $\gamma = 2$, with and without the enhancement due to GW dissipation, respectively. As a comparison, we also plot the current constraint from the microlensing search collaborations OGLE [67] and EROS [68].

It shows that LISA can probe the primordial BH abundance in a large range of masses, $[10^{-9}, 1]M_{\odot}$ for $\gamma = 2$ and $[10^{-6}, 1]M_{\odot}$ for $\gamma = 1$, respectively. We do not consider more massive primordial BHs because it may break the condition of extreme mass ratio. For primordial BHs with $1M_{\odot}$, LISA can constrain the abundance to be $\sim 10^{-6}$ ($\gamma = 1$) or $\sim 10^{-9}$ ($\gamma = 2$). The enhancement effect due to GW dissipation can further improve the constraint at the lower end of the mass range. This would be the most sensitive method proposed and quantified by now for detecting or constraining subsolar mass primordial BHs.

V. CONCLUSIONS

In this work we have investigated the SGWB from primordial BH EMRIs surrounding Sagittarius A* and the extragalactic massive BHs, respectively, expanding the previous work of Ref. [40, 41] by including the complete

extragalactic contribution. After modeling the event rate, the SGWB energy density spectra are calculated. The contributions from Sagittarius A* and extragalactic massive BHs peak at different characteristic frequencies. Future space-based GW detectors such as LISA may utilize this feature to give decisive evidence about the existence of primordial BH dark matter at the galactic center. Finally, LISA can also constrain the abundance of primordial BH in dark matter if there will be a null SGWB searching result. For a NFW induced dark-matter spike profile ($\gamma = 1$), LISA can exclude the existence of $1M_{\odot}$ primordial BH with any abundance greater than 10^{-6} of dark matter. A steeper dark-matter profile power index $\gamma = 2$ can make the constraint even tighter by three orders of magnitude. This renders GWs in the space-based frequency band a powerful tool to hunting for subsolar mass primordial BHs. However, modeling uncertainties exist from the dark-matter spike profile power index and the extragalactic massive BHs population as quantified in Section III. Future astrophysical progress on understanding these modeling systematics can help further improve the ability of the GW window to search for primordial BHs. In addition, as a future work, we will apply the specialized technique of the GW radiometer on the LISA detector to investigate the detection ability for the directional EMRI background from Sagittarius A*. It would also be interesting to study whether the stochastic background is continuous or popcorn [69, 70], thereby applying different optimal detection strategies accordingly [71].

ACKNOWLEDGMENTS

Q.-G.H. is supported by grants from NSFC (Grants No. 11690021, No. 11975019, No. 11947302, No. 11991053), the Strategic Priority Research Program of Chinese Academy of Sciences (Grants No. XDB23000000, No. XDA15020701), and Key Research Program of Frontier Sciences, CAS, Grant No. ZDBS-LY-7009. T.G.F.L. is partially supported by grants from the Research Grants Council of the Hong Kong (Project No. 24304317), Research Committee of the Chinese University of Hong Kong and the Croucher Foundation of Hong Kong.

-
- [1] B. P. Abbott *et al.* (Virgo, LIGO Scientific), “Observation of Gravitational Waves from a Binary Black Hole Merger,” *Phys. Rev. Lett.* **116**, 061102 (2016), [arXiv:1602.03837 \[gr-qc\]](#).
 - [2] B. P. Abbott *et al.* (Virgo, LIGO Scientific), “GW151226: Observation of Gravitational Waves from a 22-Solar-Mass Binary Black Hole Coalescence,” *Phys. Rev. Lett.* **116**, 241103 (2016), [arXiv:1606.04855 \[gr-qc\]](#).
 - [3] B. P. Abbott *et al.* (Virgo, LIGO Scientific), “Binary Black Hole Mergers in the first Advanced LIGO Observing Run,” *Phys. Rev.* **X6**, 041015 (2016), [arXiv:1606.04856 \[gr-qc\]](#).
 - [4] Benjamin P. Abbott *et al.* (VIRGO, LIGO Scientific), “GW170104: Observation of a 50-Solar-Mass Binary Black Hole Coalescence at Redshift 0.2,” *Phys. Rev. Lett.* **118**, 221101 (2017), [arXiv:1706.01812 \[gr-qc\]](#).

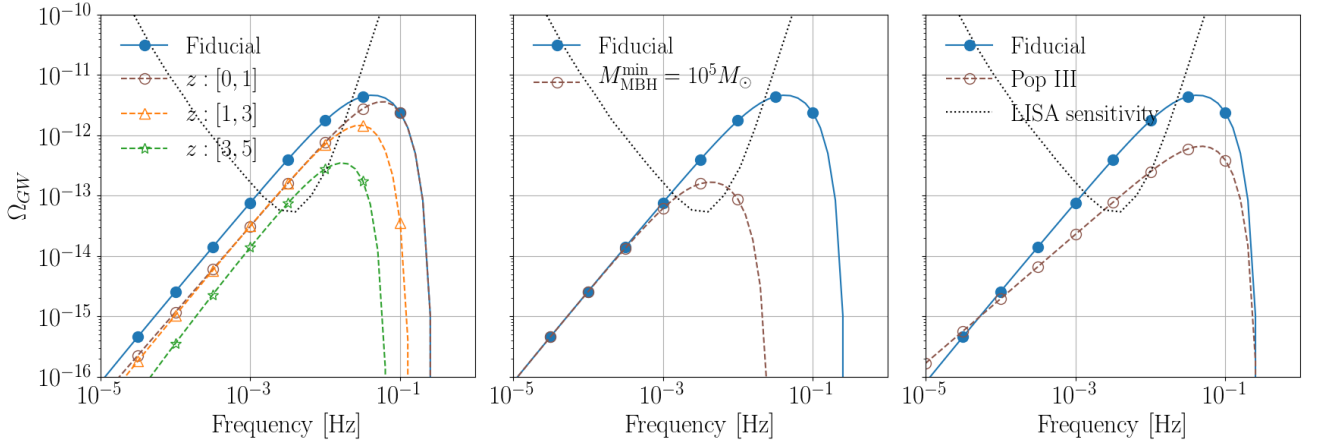


FIG. 6: The effect on SGWB spectra from the modeling systematics of massive BH. The three figures present the SGWB by varying the redshift integral limits, the lower mass of massive BHs and the massive BH population model, respectively. All SGWB spectra are calculated from $\gamma = 2$ dark-matter spike distribution and $f_{\text{PBH}} = 10^{-8}$, $m_{\text{PBH}} = 1M_\odot$.

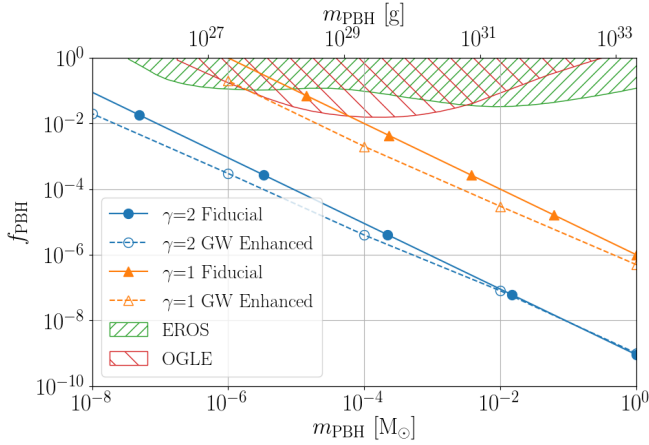


FIG. 7: The projected constraints on primordial BH abundance in dark matter with LISA for $\gamma = 1$ and $\gamma = 2$, with and without the enhancement due to GW dissipation, respectively. As a comparison, we also plot the current constraint from the microlensing search collaborations OGLE [67] and EROS [68].

- [5] B. P. Abbott *et al.* (Virgo, LIGO Scientific), “GW170814: A Three-Detector Observation of Gravitational Waves from a Binary Black Hole Coalescence,” *Phys. Rev. Lett.* **119**, 141101 (2017), [arXiv:1709.09660 \[gr-qc\]](#).
- [6] B.P. Abbott *et al.* (Virgo, LIGO Scientific), “GW170817: Observation of Gravitational Waves from a Binary Neutron Star Inspiral,” *Phys. Rev. Lett.* **119**, 161101 (2017), [arXiv:1710.05832 \[gr-qc\]](#).
- [7] B. P. Abbott *et al.* (Virgo, LIGO Scientific), “GW170608: Observation of a 19-solar-mass Binary Black Hole Coalescence,” (2017), [arXiv:1711.05578 \[astro-ph.HE\]](#).
- [8] B. P. Abbott *et al.* (LIGO Scientific, Virgo), “GWTC-1: A Gravitational-Wave Transient Catalog of Compact Binary Mergers Observed by LIGO and Virgo during the First and Second Observing Runs,” (2018), [arXiv:1811.12907 \[astro-ph.HE\]](#).

- [9] B. P. Abbott *et al.* (LIGO Scientific, Virgo), “Binary Black Hole Population Properties Inferred from the First and Second Observing Runs of Advanced LIGO and Advanced Virgo,” (2018), [arXiv:1811.12940 \[astro-ph.HE\]](#).
- [10] Simeon Bird, Ilias Cholis, Julian B. Muñoz, Yacine Ali-Haïmoud, Marc Kamionkowski, Ely D. Kovetz, Alvise Raccanelli, and Adam G. Riess, “Did ligo detect dark matter?” *Phys. Rev. Lett.* **116**, 201301 (2016).
- [11] Sebastien Clesse and Juan García-Bellido, “The clustering of massive Primordial Black Holes as Dark Matter: measuring their mass distribution with Advanced LIGO,” *Phys. Dark Univ.* **10**, 002 (2016), [arXiv:1603.05234 \[astro-ph.CO\]](#).
- [12] Misao Sasaki, Teruaki Suyama, Takahiro Tanaka, and Shuichiro Yokoyama, “Primordial Black Hole Scenario for the Gravitational-Wave Event GW150914,” *Phys. Rev. Lett.* **117**, 061101 (2016), [arXiv:1603.08338 \[astro-ph.CO\]](#).
- [13] Zu-Cheng Chen and Qing-Guo Huang, “Merger Rate Distribution of Primordial-Black-Hole Binaries,” *Astrophys. J.* **864**, 61 (2018), [arXiv:1801.10327 \[astro-ph.CO\]](#).
- [14] Stephen Hawking, “Gravitationally collapsed objects of very low mass,” *Mon. Not. Roy. Astron. Soc.* **152**, 75 (1971).
- [15] Bernard J. Carr and S. W. Hawking, “Black holes in the early Universe,” *Mon. Not. Roy. Astron. Soc.* **168**, 399–415 (1974).
- [16] Alexandre Dolgov and Joseph Silk, “Baryon isocurvature fluctuations at small scales and baryonic dark matter,” *Phys. Rev. D* **47**, 4244–4255 (1993).
- [17] Karsten Jedamzik, “Primordial black hole formation during the QCD epoch,” *Phys. Rev. D* **55**, 5871–5875 (1997), [arXiv:astro-ph/9605152 \[astro-ph\]](#).
- [18] Bernard Carr, Florian Kuhnel, and Marit Sandstad, “Primordial Black Holes as Dark Matter,” *Phys. Rev. D* **94**, 083504 (2016), [arXiv:1607.06077 \[astro-ph.CO\]](#).
- [19] Misao Sasaki, Teruaki Suyama, Takahiro Tanaka, and Shuichiro Yokoyama, “Primordial black holes—

- perspectives in gravitational wave astronomy,” *Class. Quant. Grav.* **35**, 063001 (2018), [arXiv:1801.05235 \[astro-ph.CO\]](#).
- [20] Konstantin M. Belotsky, Vyacheslav I. Dokuchaev, Yury N. Eroshenko, Ekaterina A. Esipova, Maxim Yu. Khlopov, Leonid A. Khromykh, Alexander A. Kirillov, Valeriy V. Nikulin, Sergey G. Rubin, and Igor V. Svdakovsky, “Clusters of primordial black holes,” *Eur. Phys. J.* **C79**, 246 (2019), [arXiv:1807.06590 \[astro-ph.CO\]](#).
- [21] Sergei V. Ketov and Maxim Yu. Khlopov, “Cosmological Probes of Supersymmetric Field Theory Models at Superhigh Energy Scales,” *Symmetry* **11**, 511 (2019).
- [22] Paulo Montero-Camacho, Xiao Fang, Gabriel Vazquez, Makana Silva, and Christopher M. Hirata, “Revisiting constraints on asteroid-mass primordial black holes as dark matter candidates,” *JCAP* **1908**, 031 (2019), [arXiv:1906.05950 \[astro-ph.CO\]](#).
- [23] B. P. Abbott *et al.* (LIGO Scientific, Virgo), “Search for Substellar-Mass Ultracompact Binaries in Advanced LIGO’s First Observing Run,” *Phys. Rev. Lett.* **121**, 231103 (2018), [arXiv:1808.04771 \[astro-ph.CO\]](#).
- [24] B. P. Abbott *et al.* (LIGO Scientific, Virgo), “Search for Substellar Mass Ultracompact Binaries in Advanced LIGO’s Second Observing Run,” *Phys. Rev. Lett.* **123**, 161102 (2019), [arXiv:1904.08976 \[astro-ph.CO\]](#).
- [25] John Kormendy and Luis C. Ho, “Coevolution (Or Not) of Supermassive Black Holes and Host Galaxies,” *Ann. Rev. Astron. Astrophys.* **51**, 511–653 (2013), [arXiv:1304.7762 \[astro-ph.CO\]](#).
- [26] John Kormendy and Douglas Richstone, “Inward bound: The Search for supermassive black holes in galactic nuclei,” *Ann. Rev. Astron. Astrophys.* **33**, 581 (1995).
- [27] Stanislav Babak, Jonathan Gair, Alberto Sesana, Enrico Barausse, Carlos F. Sopuerta, Christopher P. L. Berry, Emanuele Berti, Pau Amaro-Seoane, Antoine Petiteau, and Antoine Klein, “Science with the space-based interferometer LISA. V: Extreme mass-ratio inspirals,” *Phys. Rev.* **D95**, 103012 (2017), [arXiv:1703.09722 \[gr-qc\]](#).
- [28] Pau Amaro-Seoane and Miguel Preto, “The impact of realistic models of mass segregation on the event rate of extreme-mass ratio inspirals and cusp re-growth,” *Laser interferometer space antenna. Proceedings, 8th International LISA Symposium, Stanford, USA, June 28–July 2, 2010*, *Class. Quant. Grav.* **28**, 094017 (2011), [arXiv:1010.5781 \[astro-ph.CO\]](#).
- [29] Leor Barack and Curt Cutler, “Using LISA EMRI sources to test off-Kerr deviations in the geometry of massive black holes,” *Phys. Rev.* **D75**, 042003 (2007), [arXiv:gr-qc/0612029 \[gr-qc\]](#).
- [30] Jonathan R. Gair, Michele Vallisneri, Shane L. Larson, and John G. Baker, “Testing General Relativity with Low-Frequency, Space-Based Gravitational-Wave Detectors,” *Living Rev. Rel.* **16**, 7 (2013), [arXiv:1212.5575 \[gr-qc\]](#).
- [31] Tania Regimbau, “The astrophysical gravitational wave stochastic background,” *Res. Astron. Astrophys.* **11**, 369–390 (2011), [arXiv:1101.2762 \[astro-ph.CO\]](#).
- [32] Joseph D. Romano and Neil J. Cornish, “Detection methods for stochastic gravitational-wave backgrounds: a unified treatment,” *Living Reviews in Relativity* **20**, 2 (2017).
- [33] B. P. Abbott *et al.* (Virgo, LIGO Scientific), “GW150914: Implications for the stochastic gravitational wave background from binary black holes,” *Phys. Rev. Lett.* **116**, 131102 (2016), [arXiv:1602.03847 \[gr-qc\]](#).
- [34] Benjamin P. Abbott *et al.* (Virgo, LIGO Scientific), “Upper Limits on the Stochastic Gravitational-Wave Background from Advanced LIGO’s First Observing Run,” *Phys. Rev. Lett.* **118**, 121101 (2017), [arXiv:1612.02029 \[gr-qc\]](#).
- [35] Benjamin P. Abbott *et al.* (Virgo, LIGO Scientific), “GW170817: Implications for the Stochastic Gravitational-Wave Background from Compact Binary Coalescences,” *Phys. Rev. Lett.* **120**, 091101 (2018), [arXiv:1710.05837 \[gr-qc\]](#).
- [36] Vuk Mandic, Simeon Bird, and Ilias Cholis, “Stochastic Gravitational-Wave Background due to Primordial Binary Black Hole Mergers,” *Phys. Rev. Lett.* **117**, 201102 (2016), [arXiv:1608.06699 \[astro-ph.CO\]](#).
- [37] Sai Wang, Yi-Fan Wang, Qing-Guo Huang, and Tjonnie G. F. Li, “Constraints on the Primordial Black Hole Abundance from the First Advanced LIGO Observation Run Using the Stochastic Gravitational-Wave Background,” *Phys. Rev. Lett.* **120**, 191102 (2018), [arXiv:1610.08725 \[astro-ph.CO\]](#).
- [38] Zu-Cheng Chen, Fan Huang, and Qing-Guo Huang, “Stochastic Gravitational-Wave Background from Binary Black Holes and Binary Neutron Stars,” (2018), [arXiv:1809.10360 \[gr-qc\]](#).
- [39] Sebastien Clesse and Juan García-Bellido, “Detecting the gravitational wave background from primordial black hole dark matter,” (2016), [arXiv:1610.08479 \[astro-ph.CO\]](#).
- [40] Florian Kühnel, Glenn D. Starkman, and Katherine Freese, “Primordial Black-Hole and Macroscopic Dark-Matter Constraints with LISA,” (2017), [arXiv:1705.10361 \[gr-qc\]](#).
- [41] Florian Kühnel, Andrew Matas, Glenn D. Starkman, and Katherine Freese, “Waves from the Centre: Probing PBH and other Macroscopic Dark Matter with LISA,” (2018), [arXiv:1811.06387 \[gr-qc\]](#).
- [42] Paolo Gondolo and Joseph Silk, “Dark matter annihilation at the galactic center,” *Phys. Rev. Lett.* **83**, 1719–1722 (1999).
- [43] Hiroya Nishikawa, Ely D. Kovetz, Marc Kamionkowski, and Joseph Silk, “Primordial-black-hole mergers in dark-matter spikes,” (2017), [arXiv:1708.08449 \[astro-ph.CO\]](#).
- [44] Julio F. Navarro, Carlos S. Frenk, and Simon D. M. White, “The Structure of cold dark matter halos,” *Astrophys. J.* **462**, 563–575 (1996), [arXiv:astro-ph/9508025 \[astro-ph\]](#).
- [45] Aaron A. Dutton and Andrea V. Macciò, “Cold dark matter haloes in the Planck era: evolution of structural parameters for Einasto and NFW profiles,” *Mon. Not. Roy. Astron. Soc.* **441**, 3359–3374 (2014), [arXiv:1402.7073 \[astro-ph.CO\]](#).
- [46] P. A. R. Ade *et al.* (Planck), “Planck 2013 results. XVI. Cosmological parameters,” *Astron. Astrophys.* **571**, A16 (2014), [arXiv:1303.5076 \[astro-ph.CO\]](#).
- [47] Darren J. Croton, “A simple model to link the properties of quasars to the properties of dark matter halos out to high redshift,” *Mon. Not. Roy. Astron. Soc.* **394**, 1109–1119 (2009), [arXiv:0901.4104 \[astro-ph.CO\]](#).
- [48] P. C. Peters and J. Mathews, “Gravitational radiation from point masses in a keplerian orbit,” *Phys. Rev.* **131**, 435–440 (1963).
- [49] P. C. Peters, “Gravitational radiation and the motion of two point masses,” *Phys. Rev.* **136**, B1224–B1232 (1964).

- [50] Chiara Caprini *et al.*, “Science with the space-based interferometer eLISA. II: Gravitational waves from cosmological phase transitions,” *JCAP* **1604**, 001 (2016), [arXiv:1512.06239 \[astro-ph.CO\]](#).
- [51] Nicola Bartolo *et al.*, “Science with the space-based interferometer LISA. IV: Probing inflation with gravitational waves,” *JCAP* **1612**, 026 (2016), [arXiv:1610.06481 \[astro-ph.CO\]](#).
- [52] Stefan W. Ballmer, “A Radiometer for stochastic gravitational waves,” *Gravitational waves. Proceedings, 6th Edoardo Amaldi Conference, Amaldi6, Bankoku Shinryoukan, June 20-24, 2005*, *Class. Quant. Grav.* **23**, S179–S186 (2006), [arXiv:gr-qc/0510096 \[gr-qc\]](#).
- [53] B. P. Abbott *et al.* (LIGO Scientific, Virgo), “Directional limits on persistent gravitational waves using data from Advanced LIGO’s first two observing runs,” *Phys. Rev. D* **100**, 062001 (2019), [arXiv:1903.08844 \[gr-qc\]](#).
- [54] Benjamin P. Abbott *et al.* (LIGO Scientific, Virgo), “Directional Limits on Persistent Gravitational Waves from Advanced LIGOs First Observing Run,” *Phys. Rev. Lett.* **118**, 121102 (2017), [arXiv:1612.02030 \[gr-qc\]](#).
- [55] J. Abadie *et al.* (LIGO Scientific), “Directional limits on persistent gravitational waves using LIGO S5 science data,” *Phys. Rev. Lett.* **107**, 271102 (2011), [arXiv:1109.1809 \[astro-ph.CO\]](#).
- [56] Carlo Ungarelli and Alberto Vecchio, “Studying the anisotropy of the gravitational wave stochastic background with LISA,” *Phys. Rev. D* **64**, 121501 (2001), [arXiv:astro-ph/0106538 \[astro-ph\]](#).
- [57] Hideaki Kudoh, Atsushi Taruya, Takashi Hiramatsu, and Yoshiaki Himemoto, “Detecting a gravitational-wave background with next-generation space interferometers,” *Phys. Rev. D* **73**, 064006 (2006), [arXiv:gr-qc/0511145 \[gr-qc\]](#).
- [58] Darren Reed, Richard Bower, Carlos Frenk, Adrian Jenkins, and Tom Theuns, “The halo mass function from the dark ages through the present day,” *Mon. Not. Roy. Astron. Soc.* **374**, 2–15 (2007), [arXiv:astro-ph/0607150 \[astro-ph\]](#).
- [59] Steven Murray, Chris Power, and Aaron Robotham, “HMFcalc: An Online Tool for Calculating Dark Matter Halo Mass Functions,” (2013), [arXiv:1306.6721 \[astro-ph.CO\]](#).
- [60] N. Aghanim *et al.* (Planck), “Planck 2018 results. VI. Cosmological parameters,” (2018), [arXiv:1807.06209 \[astro-ph.CO\]](#).
- [61] Jong-Hak Woo, Hojin Cho, Elena Gallo, Edmund Hodges-Kluck, Huynh Anh N. Le, Jaejin Shin, Donghoon Son, and John C. Horst, “A 10,000-solar-mass black hole in the nucleus of a bulgeless dwarf galaxy,” *Nature Astronomy* **3**, 755–759 (2019), [arXiv:1905.00145 \[astro-ph.GA\]](#).
- [62] Hidenobu Yajima, Kentaro Nagamine, Qirong Zhu, Sadegh Khochfar, and Claudio Dalla Vecchia, “Growth of First Galaxies: Impacts of Star Formation and Stellar Feedback,” *Astrophys. J.* **846**, 30 (2017), [arXiv:1704.03117 \[astro-ph.GA\]](#).
- [63] Enrico Barausse, “The evolution of massive black holes and their spins in their galactic hosts,” *Mon. Not. Roy. Astron. Soc.* **423**, 2533–2557 (2012), [arXiv:1201.5888 \[astro-ph.CO\]](#).
- [64] A. Sesana, E. Barausse, M. Dotti, and E. M. Rossi, “Linking the spin evolution of massive black holes to galaxy kinematics,” *Astrophys. J.* **794**, 104 (2014), [arXiv:1402.7088 \[astro-ph.CO\]](#).
- [65] Fabio Antonini, Enrico Barausse, and Joseph Silk, “The imprint of massive black-hole mergers on the correlation between nuclear star clusters and their host galaxies,” *Astrophys. J.* **806**, L8 (2015), [arXiv:1504.04033 \[astro-ph.GA\]](#).
- [66] Fabio Antonini, Enrico Barausse, and Joseph Silk, “The Coevolution of Nuclear Star Clusters, Massive Black Holes, and their Host Galaxies,” *Astrophys. J.* **812**, 72 (2015), [arXiv:1506.02050 \[astro-ph.GA\]](#).
- [67] Hiroko Niihara, Masahiro Takada, Shuichiro Yokoyama, Takahiro Sumi, and Shogo Masaki, “Constraints on Earth-mass primordial black holes from OGLE 5-year microlensing events,” *Phys. Rev. D* **99**, 083503 (2019), [arXiv:1901.07120 \[astro-ph.CO\]](#).
- [68] P. Tisserand *et al.* (EROS-2), “Limits on the Macho Content of the Galactic Halo from the EROS-2 Survey of the Magellanic Clouds,” *Astron. Astrophys.* **469**, 387–404 (2007), [arXiv:astro-ph/0607207 \[astro-ph\]](#).
- [69] Pablo A. Rosado, “Gravitational wave background from binary systems,” *Phys. Rev. D* **84**, 084004 (2011), [arXiv:1106.5795 \[gr-qc\]](#).
- [70] T. Regimbau and Scott A. Hughes, “Confusion background from compact binaries,” *Gravitational waves. Proceedings, 8th Edoardo Amaldi Conference, Amaldi 8, New York, USA, June 22-26, 2009*, *J. Phys. Conf. Ser.* **228**, 012009 (2010), [arXiv:0911.1043 \[gr-qc\]](#).
- [71] Rory Smith and Eric Thrane, “Optimal search for an astrophysical gravitational-wave background,” *Phys. Rev. X* **8**, 021019 (2018).